

**Supplementary Information for**

**A New Method to Assay Protease Based on Amyloid Misfolding:**

**Application to Prostate Cancer Diagnosis Using a Panel of Proteases**

**Biomarkers**

Hao Li<sup>1</sup>, Yue Huang<sup>1</sup>, Bin Zhang<sup>2</sup>, Dawei Yang<sup>1</sup>, Xiaoli Zhu<sup>2</sup>, Genxi Li<sup>1,2,\*</sup>

1. Department of Biochemistry and State Key Laboratory of Pharmaceutical Biotechnology,

Nanjing University, Nanjing, China.

2. Laboratory of Biosensing Technology, School of Life Sciences, Shanghai University, Shanghai,

China.

\*Corresponding author at Department of Biochemistry and State Key Laboratory of Pharmaceutical Biotechnology, Nanjing University, Nanjing 210093, China. Fax: +86 25 83592510. E-mail address: genxili@nju.edu.cn.

## Validation of the proposed mechanism of protease detection

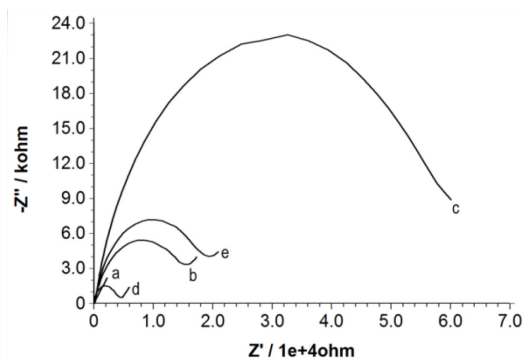


**Figure S1.** EIS recorded after every step of the assay, (a) the bare electrode, (b) the electrode after immobilization of peptide probe, (c) in the absence of matriptase and after amyloid-beta misfolding, (d) in the presence of matriptase, (e) in the presence of matriptase, the peptide-modified electrode is firstly cleavage by matriptase and then undergoes amyloid-beta misfolding step.

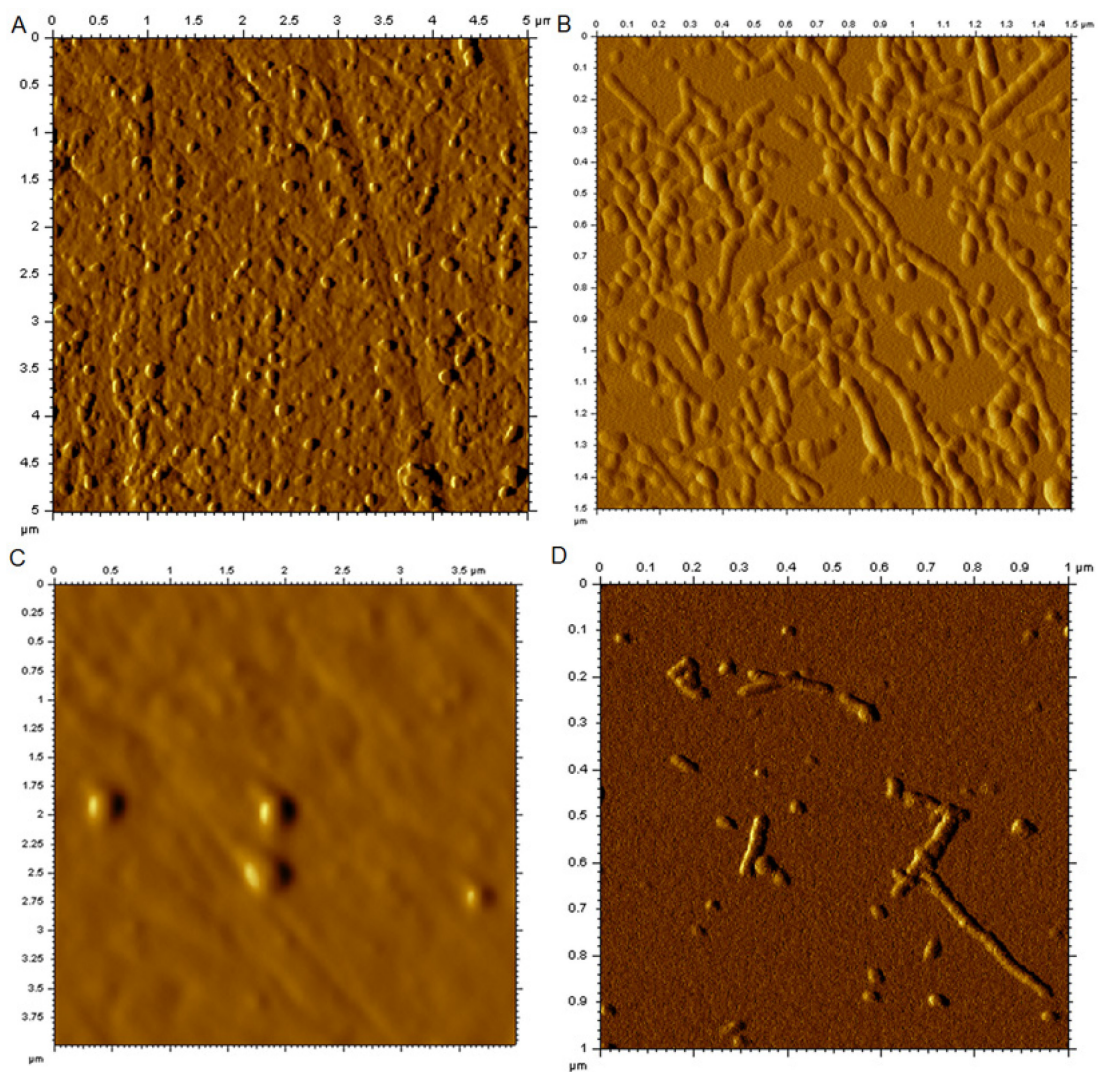


**Figure S2.** AFM images obtained at the peptide-modified electrode under various conditions.

### Optimization of experimental conditions

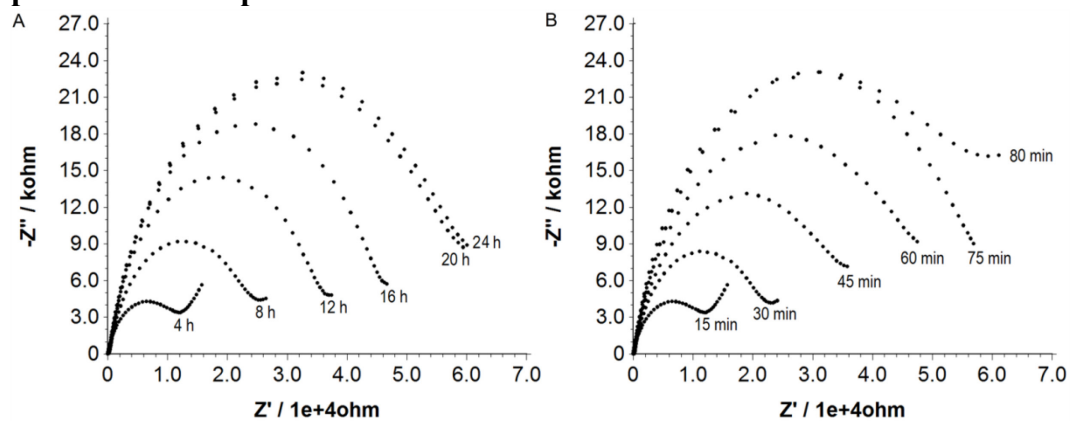


**Figure S3.** EIS obtained at the peptide-modified electrode to show the influence of peroxyntirite on amyloid-beta misfolding. (A) and (B) are separately the cases of amyloid-beta misfolding in the absence/presence of 100  $\mu\text{M}$  peroxyntirite.

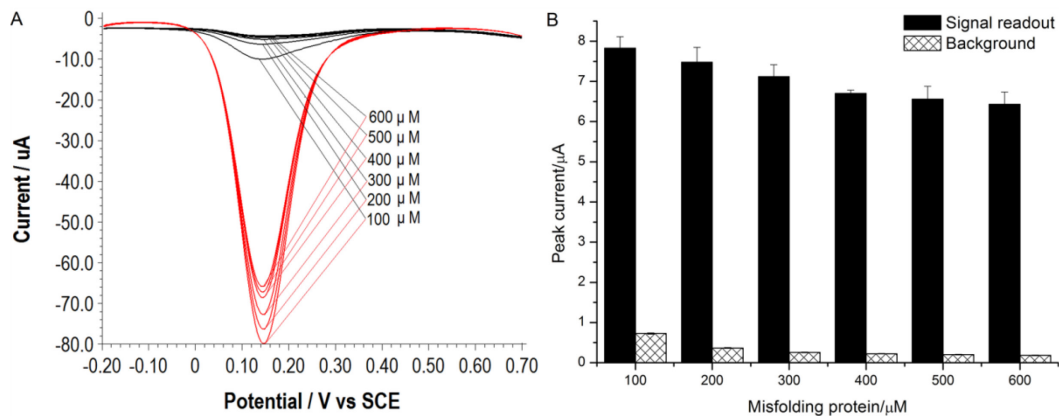


**Figure S4.** (A) Square wave voltammograms (SWVs) of  $[\text{Fe}(\text{CN})_6]^{3-/4-}$  to optimize the concentration of amyloid-beta monomer. The red and the black curves are obtained in the presence/absence of matriptase, respectively. (B) Influence of the concentration of amyloid-beta monomer on the obtained signal and background. The error bars represent standard deviation from average (n=3).

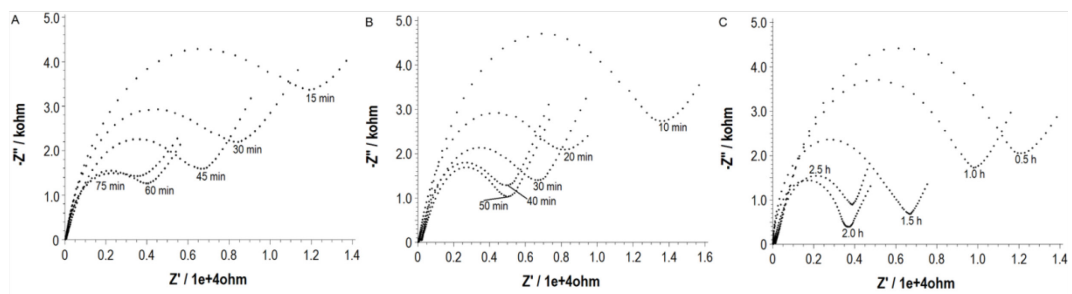


**Figure S5.** EIS obtained at the peptide-modified electrode showing the influence of cleavage time for (A) matriptase, (B) kallikrein 2 and (C) PSA.

## Specificity of the protease assay

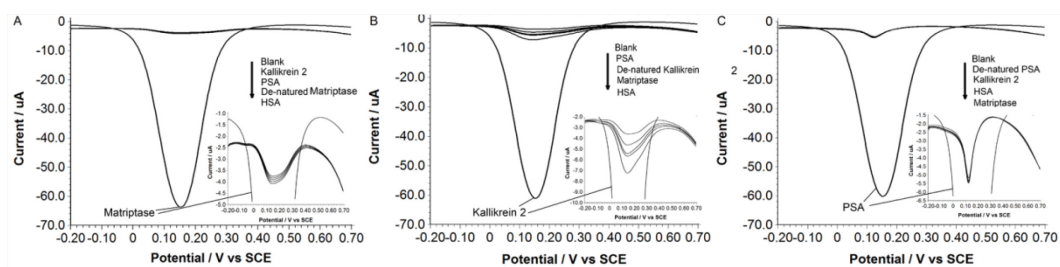


**Figure S6.** SWVs of  $[\text{Fe}(\text{CN})_6]^{3-/4-}$  to show the specificity of our method in the detection of (A) matriptase, (B) kallikrein 2 and (C) PSA, all the control species are at 1000 pM concentration. Inset is the enlarged view of control species.

**Table S1.** Comparison between Our Method and Commercially Available ELISA Kits

<b>Matriptase</b>	Detection range	Limit of detection	Recovery
The proposed assay	0.1 – 398 pM	0.047 pM	106%
ELISA kit [1]	0.2 – 11.2 nM	0.04 nM	No data

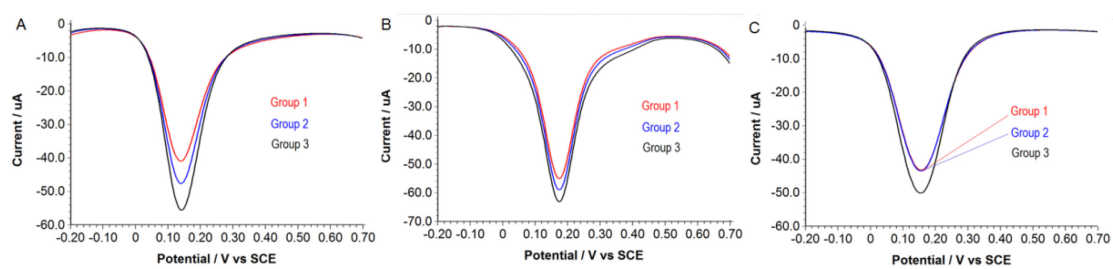
  

<b>Kallikrein 2</b>	Detection range	Limit of detection	Recovery
The proposed assay	0.1 – 1000 pM	0.035 pM	102%
ELISA kit [2]	3.9 – 250 nM	1.45 pM	89%

<b>PSA</b>	Detection range	Limit of detection	Recovery
The proposed assay	0.1 – 320 pM	0.067 pM	104%
ELISA kit [3]	0.28 – 68.4 pM	0.22 pM	105.4%

## Protease assay in patient serum sample



**Figure S7.** SWVs of  $[\text{Fe}(\text{CN})_6]^{3-/4-}$  obtained at (A) matriptase-, (B) kallikrein 2- and (C) PSA-specific peptide probe modified electrodes to show the typical square wave voltammetric response of patient serum samples in detecting the respective protease. The groups indicated are based on the data distribution shown in Figure 4.

## Validation of the proposed peptide probe

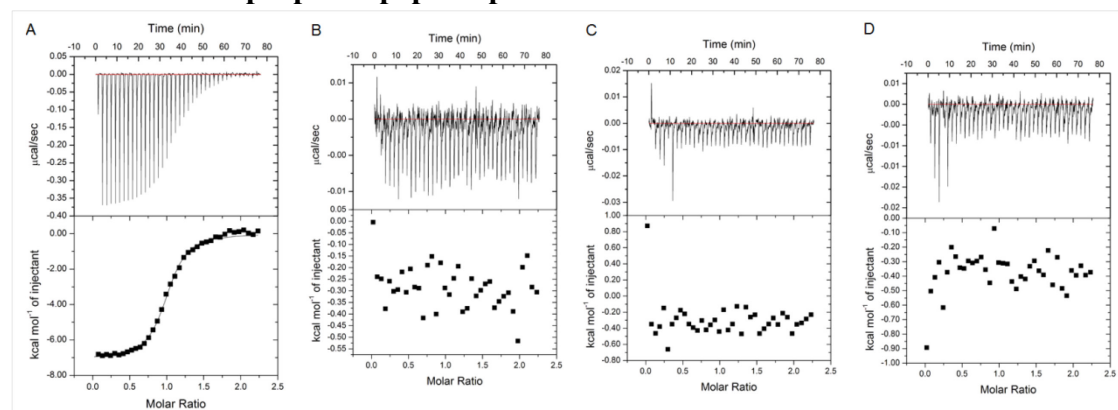


**Figure S8.** (A) ~ (C): ITC data of 0.55 mM peptide probe (SGKGSSGSSTRQARVK LVFFEEEE) titrated into 0.05 mM matriptase, plasmin and thrombin, respectively, at 25°C in 100 mM Tris (pH 7.0), pH 7.0 is adopted to prevent cleavage of the peptide by the enzyme. (D) ITC data of 1 mM HSA titrated into 0.05 mM peptide probe. The top row displays the raw data of power versus time. The bottom row are corresponding data by integrating enthalpy values versus the molar ratio of tritand:tritrant. These data are fit to the “one-site binding model” using Origin 7.0 software, the resulted fitting curve is also shown in (A).

As shown by the titrations and the fitting, only matriptase has specific interaction with the peptide probe (table S2), although the concentration of control proteins is greater than their respective serum concentration [4-6]. Binding between the probe and its target enzyme is moderately strong and slightly entropically favorable. Therefore, the probe can specifically recognize its target protease, while the interaction is not so strong as to hinder the rapid turnover of substrate.

**Table S2.** Thermodynamic Binding Data for Peptide Probe/matriptase Interaction

n	K (M <sup>-1</sup> )	ΔG (kcal/mol)	ΔH (kcal/mol)	ΔS (cal/mol/deg)
0.995 ± 0.005	(1.04 ± 0.08) × 10 <sup>6</sup>	-8.38 (± 0.18)	-7.08 (± 0.06)	3.78 (± 0.21)

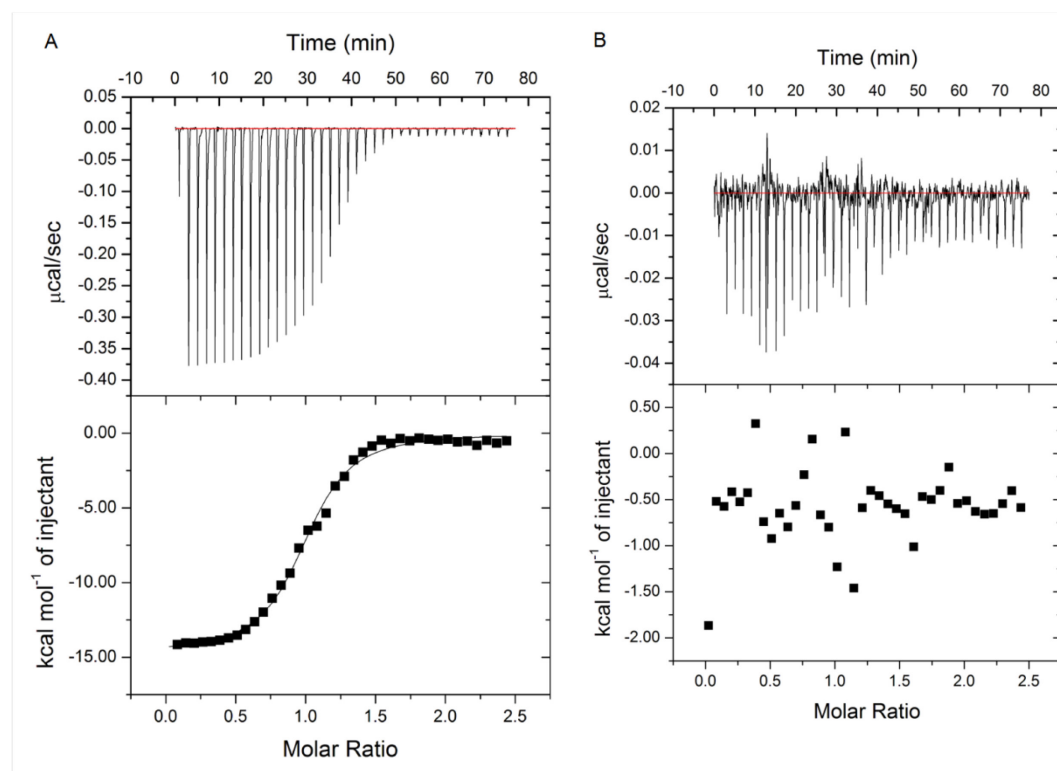


**Figure S9.** ITC data of the peptide probe (A) and a control peptide (B) without the amyloid-beta binding sequence (SGKGSSGSSTRQARV) titrated into amyloid-beta monomer in 100mM Tris (pH 7.0), pH 7.0 is adopted to prevent rapid aggregation of amyloid-beta. The peptide probe is titrated at 0.3 mM into a 0.025 mM solution of amyloid-beta monomer. The top row displays the raw data of power versus time. The bottom row are corresponding data by integrating enthalpy values versus the molar ratio of titrant:titrand. These data are fit to the “one-site binding model” using Origin 7.0 software, the resulted fitting curve is also shown in (A).

As shown by the titrations and the fitting, only the full length probe has specific interaction with amyloid-beta (table S3). Binding between the probe and amyloid-beta is enthalpy-driven and entropically unfavorable, indicating that specific electrostatic interaction between the probe and amyloid-beta has induced conformational change upon binding.

**Table S3.** Thermodynamic Binding Data for Peptide Probe/amyloid-beta Interaction

n	K (M <sup>-1</sup> )	ΔG (kcal/mol)	ΔH (kcal/mol)	ΔS (cal/mol/deg)
0.995 ± 0.008	(1.37 ± 0.05) × 10 <sup>6</sup>	-8.39 (± 0.16)	-14.71 (± 0.17)	-21.20 (± 0.53)

### Anti-fouling effect of the absorption-resistant peptide

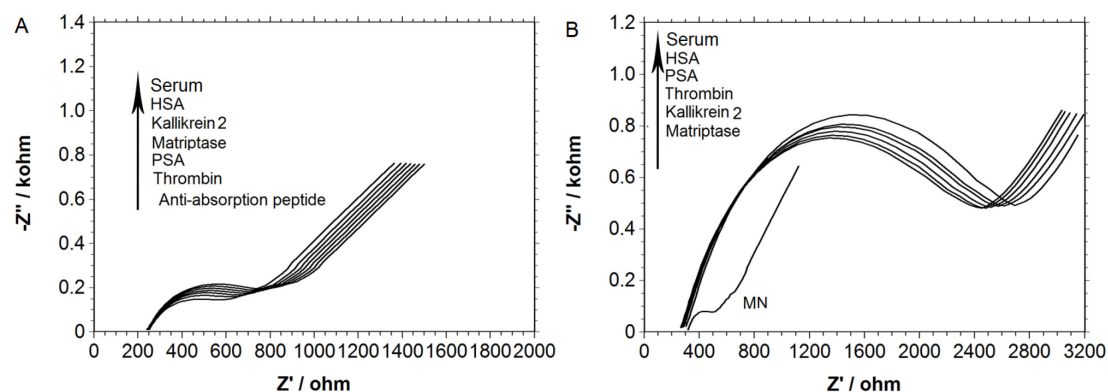


**Figure S10.** EIS obtained at (A) 9-mercaptononanol (MN)-modified and (B) absorption-resistant peptide (MUA-SGKGSSGSST)-modified electrode after 1 h incubation at room temperature with serum of healthy volunteer, or 1mM HSA, or 0.05 mM various other serum proteins as indicated in the figure.

As shown in Figure S10A, the anti-fouling effect of the absorption-resistant peptide is satisfactory since the absorption induced impedance is negligible in comparison to the impedance induced by amyloid-beta misfolding, as shown in Figure S1. As a comparison, the commonly employed passivation reagent, MN shows greater absorption that may lead to false negative (Figure S10B), so we have employed the peptide as the passivation reagent to minimize fouling from the serum sample in this study.

## Reference

1. [Internet] <http://www.enzolifesciences.com/ADI-900-221/matriptase-human-elisa-kit/>
2. [Internet] <http://www.uscnk.de/en/products/detail/nr/uscn-life-science--elisa-kit--hu--e93108hu--elisa-kit-for-kallikrein-2-klk2.html>
3. [Internet] <http://www.abcam.cn/psa-klk3nbsphuman-elisa-kit-ab113327.html>
4. Frank P, The plasma proteins (second edition) structure, function, and genetic control. Orlando, USA: Academic press; 1984.
5. Wohl RC, Sinio L, Robbins KC, Methods for studying fibrinolytic pathway components in human plasma. Throm Res. 1984; 27: 523-535.
6. Fasano M, Curry S, Terreno E, et. al. The extraordinary ligand binding properties of human serum albumin. IUBMB Life. 2005; 57: 787-796.